MEASURING THE VARIABILITY OF EVENT-RELATED BOLD SIGNAL

J.-R. Duann, T.-P. Jung, W.-J. Kuo, T.-C. Yeh, S. Makeig, J.-C. Hsieh, T. J. Sejnowski

Computational Neurobiology Lab, the Salk Institute for Biological Studies, CA 92037, USA
Institute for Neural Computation, University of California, San Diego
Integrated Brain Research Unit, Taipei-Veterans General Hospital, Taipei, Taiwan, ROC

ABSTRACT

Most current analysis methods for functional magnetic resonance imaging (fMRI) data assume *a priori* knowledge of the time course of the hemodynamic response (HR) to experimental stimuli or events in brain areas of interest. In addition, they typically assume homogeneity of both the HR and the non-HR "noise" signals both across brain regions and across similar experimental events. When HRs vary unpredictably from area to area, or from trial to trial, different approaches are needed. Here we used infomax Independent Component Analysis (ICA) to detect and visualize variations in single-trial HRs in event-related fMRI data. ICA decomposition of the resulting BOLD data produced independent components with variable stimulus-locked HRs active in primary visual (V1) and medial temporal (MT/V5) cortices respectively. Contrary to expectation, in four of six subjects the HR of the V1 component contained two positive peaks in response to short-stimulus bursts, while nearly identical component maps were associated with single-peaked HRs in long-stimulus sessions from the same subject. Thus, ICA combined with single-trial visualization can reveal dramatic and unforeseen task-related HR variation not apparent to researchers analyzing the data with fixed HR templates.

1. INTRODUCTION

Although functional magnetic resonance imaging (fMRI) of blood oxygen level-dependent (BOLD) contrast allows localization of dynamic brain processes that occur during a wide range of psychological tasks [1-4], fMRI data include a complex mixture of signals resulting from hemodynamic, neural, respiratory, movement-related, temperature drift, machine-noise and other processes. A number of methods have been proposed for analyzing BOLD data. These can be categorized as hypothesis-driven and model-based or else exploratory and data-driven [5,6]. Model-based methods include ANOVA and correlational methods. Data-driven methods include principal component analysis (PCA) [7] and independent component analysis (ICA) [8-10].

Model-based methods usually assume that the shapes but not the amplitudes of the time courses of the different processes that sum to create the observed BOLD signals can be reliably estimated prior to analysis. Typically, the time course of stimulus presentation or task variation is convolved with a gamma, Poisson or Gaussian response kernel, or else a combination of Fourier series are used to generate one or more expected hemodynamic response (HR) functions [11-13]. The actual time courses of every voxel or smoothed voxel region are then compared to the selected template(s), and statistical models are used to identify regions whose time courses are significantly correlated to the models and to determine the magnitudes of their model-related activation [14-16]. In addition, it is usually assumed that the time course of the HR is constant across stimulus or task events and, often, across brain areas, stimulus parameters, sessions and subjects.

Hypothesis-driven methods may be problematic when the HR time courses of interest cannot be modeled with certainty prior to the analysis. Recorded fMRI signals consist of changes in oxygenated hemoglobin concentration both in the capillary bed of each local cortical area and in its venous drainage [17]. Since the drainage compartment may be located some distance from the capillary compartment, it may have a different BOLD time course [18-20] making it difficult to construct accurate *a priori* HR templates. Variations in HR peak latency of up to 4 s are also reported, without physiological explanation, in different regions [21]. In general, the basic model of the HR as a passive low-pass filter may have limited validity.

Some research groups have therefore begun to search for new, more flexible template-based methods for extracting accurate fMRI time courses, or for data-driven methods for adjusting *a priori* HR models to the data. Williams et al. used orienting responses (event-related changes in heart rate, EEG desynchronization, eye movement, and skin conductance) to refine their HR model [22]. Andino et al. utilized Renyi numbers of time/frequency representations on clusters of voxel time courses to measure their signal complexity and task-related information content [23]. Clare et al. demonstrated an analysis of variance (ANOVA) method for analyzing fMRI data that calculates the ratio of the variance of the averaged data set to the variance of the unaveraged data set for each voxel in the volume image [24]. Voxels in regions of activation, they reasoned, should have a significantly higher variance ratio than those in regions of purely random amplitudes. Although these methods may use less rigid assumptions about HR wave shape and timing than simple correlation methods, they assume that the same HR is evoked in each trial, and model trial-to-trial variability as statistical noise.

Although PCA, the best-known data-driven algorithm, is often employed to reduce the dimensionality of fMRI data, individual PCA components are necessarily both spatially and temporally uncorrelated, making them unlikely to represent functionally distinct brain systems. Rotation methods such as Varimax and Promax [25] might be used to relax the rigid PCA component restrictions, but their use for fMRI analysis has not been explored.

Recently McKeown and colleagues [8-10] reported a less artificially restrictive data-driven method, ICA, for blind source separation of many types of activity from fMRI data based on an information-maximization (infomax) approach [26]. Applied to fMRI data, the components found by ICA are spatially maximally independent of one another, while their time courses may be highly correlated. This approach is based on the well-established principle of functional brain modularity (different parts of the brain do different things), yet is capable of distinguishing areas having only slightly differing time courses.

ICA attempts to decompose the entire fMRI data set into component activities associated with fixed spatial distributions. Variability in the data is modeled as a sum of deterministic processes with maximally independent spatial distributions. McKeown et al. showed that ICA can distinguish and separate

activity in brain regions having consistently task-related HRs from those whose HRs are only transiently task-related [9]. ICA can also isolate other metabolic and artifactual processes, such as radio frequency (RF) noise, subject movements and arterial pulsations, that are present in the fMRI data. Because of its greater dimensionality and the non-Gaussian distributions of the derived components, ICA may have increased statistical power over standard correlation-based methods for determining the extent of task-related activity. This paper demonstrates that ICA, applied to event-related fMRI paradigms, can reveal the time courses and associated spatial locations of BOLD processes with novel and variable HRs, allowing detailed examination of HR variations across trials, sessions, sites and subjects. It demonstrates as well that may have unexpected variability, even in primary sensory areas.

2. METHOD

Subjects

Two male and four female subjects (ages: 22 ± 3 years, mean ± SD) were recruited from the academic environment of the National Yang Ming University in Taipei, Taiwan. Each subject had normal or corrected-to-normal vision. Written informed consent was obtained from each subject prior to the experiment.

Experimental Protocol

The overview of the experimental design is given in Figure 1. An 8-Hz flickering checkerboard visual stimulation was used to trigger hemodynamic responses (HRs) in visual cortical regions of each subject. Each 5-min experimental session consisted of ten 30-sec epochs beginning with a burst of visual stimulation (an event-related fMRI experimental design). In the periods between stimulus bursts, subjects were requested to fix

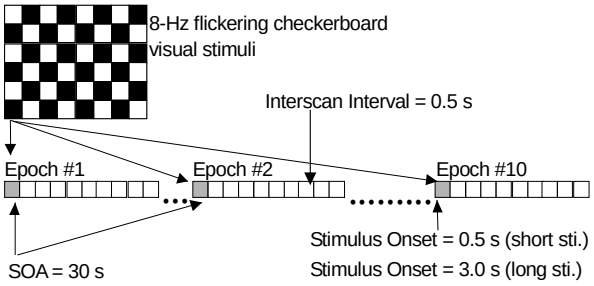

Figure 1. An event-related fMRI experimental design was used. Visual 8-Hz flickering-checkerboard stimuli were presented at the beginning of every epoch. The period of presentation was 0.5 s in short-stimulus sessions and 3 s in long-stimulus sessions. Each session comprised ten 30-sec epochs. Six subjects participated in 2 short-stimulus and 2 long-stimulus sessions.

their eyes on a red crosshair displayed in the center of visual field. Visual stimuli were presented through back projection from a LCD projector onto a white screen. Subjects lay on their backs in the bore of the scanner and viewed the screen through eyeglasses containing an angled mirror in front of each eye. The fMRI sessions were either short-stimulus (SS) sessions, in which stimulus burst duration was 0.5-s, or long-stimulus (LS) sessions in which burst durations were 3 s. Each subject participated in two LS and two SS sessions. Stimulus duration was counter-balanced over sessions and subjects to avoid order effects. A 30-s stimulus onset asynchrony (SOA) was chosen to minimize the possibility of HR overlap [27-30].

Image Acquisition

The fMR images in this study were obtained by a 3-Tesla Medspec 30/100 scanner (Bruker Medizintechnik GmbH, Ettlingen, Germany) at the Integrated Brain Research Unit (IBRU) of Taipei-Veterans General Hospital, Taipei, Taiwan. Five axial slices were acquired using an echo-planar imaging (EPI) protocol (TR = 500 ms; TE = 70 ms; flip angle = 90 degrees; matrix = 64×64; FOV = 250×250 mm; slice thickness = 5 mm with 2-mm gap). For better visualization of the active brain areas, 256×256 T1-weighted images with the same slice position and field of view as the functional images were acquired at the end of the four experimental sessions.

Data Preprocessing

The obtained fMRI images were first subjected to a slice time-alignment process to minimize image intensity inhomogeneity arising from differences in slice image acquisition timing. In this process, data from individual slices were first interpolated in time. Then, the data were sampled at a single set of time points separated by the original 500-ms TR. If left uncorrected, the staggered acquisition times for the different slices might have introduced considerable variability and timing bias into the recovered HRs [21]. The time-realigned fMRI images were then stripped of off-brain voxels by using intensity histograms of the structural images to determine the coordinates of voxels lying outside the brain. This process reduced data size by more than 60%. Independent component analysis was then applied to BOLD-signal time series of within-brain voxels to separate maximally independent brain maps and associated BOLD-signal time courses.

The ICA unmixing matrix for each fMRI session was computed using a binary version of the *runica()* routine (available online in MATLAB and binary form in [31]). PCA preprocessing was applied to reduce the dimension of training data set from 600 (the number of time points) to 50. The initial learning rate was 0.0001. Block size was 34. The complete procedure (including preprocessing) required 30 minutes to converge on a 500 MHz Pentium 4 machine. After the ICA training converged, (i.e., the unmixing matrix was determined within the pre-set tolerance), the spatially independent component maps were derived as in eq. (1). Each component map was then converted to a z-value map by subtracting its mean from each voxel and dividing by the standard deviation of the map weights. The voxels with high z values ($|z| > 2$) were considered to comprise the active component map or comprising the component region of activity (ROA).

Talairach Normalization

To visualize the ROA of each component within the high-resolution structural image, and to compare ROAs across subjects, the structural images and component maps were normalized to the standard Talairach space using statistical parametric mapping (SPM) software from the SPM99b package [5]. Selected active component maps were then overlaid onto the structural images using the *slice_display()* routine developed by Matthew Brett for SPM environment (see Figure 2). The coordinates in Talairach space of active brain areas were then obtained by locating the voxel with the largest z score in each ROA voxel cluster of interest. The Brodmann area(s) of the ROA cluster was also determined from an online atlas. Components with ROAs located in Brodmann areas 17, 18, or 19 were selected for further visualization and comparison.

BOLD-Image Plots

To display the time course of each independent component in each session, we used a new visualization tool that we call the "BOLD-image" plot after a similar plotting method, for event-related EEG data visualization, the ERP-image [25,32]. The time course of activation of each component was first

converted to regional percent signal change (RPSC) by dividing the mean back-projected component time course in the component ROA by the mean BOLD signal level in the ROA. The component time course in the 10 trials was then represented as a series of ten normalized lines or bars variably-colored according to the regional percent signal change at each time point and stacked in time order of acquisition to form a BOLD-image plot (Fig 2b). For convenience, the average time course across the ten trials was computed and drawn below the BOLD image. BOLD-image plots can effectively visualize the variability of single voxel, region-of-interest (ROI) or component ROA time courses across trials from event-related paradigms, allowing easy detection of response variations across trials or sessions.

Reproducibility within Subjects

Within the same subject, the percentage overlap ratio (O_R) of the ROAs of similar components in two different sessions was derived as

$$O_R \leq 100 \times N(ROA_1 \cap ROA_2) \Big/ \sqrt{N(ROA_1) \times N(ROA_2)} \quad (4)$$

where N(***S***) is the number of elements in set ***S***, sqrt(•) is the square root, and $\boldsymbol{ROA_1}$ and $\boldsymbol{ROA_2}$ are the sets of voxels in the ROAs of the two components or sessions. O_R can be used to measure, for example, the percentage of active voxels in a component ROA from one session decomposition that are also in the ROA of a component from the another session decomposition. Presumably, if the same brain region exhibits spatially coherent activity during different sessions, ICA should be able to find the same active component map in each session. Consequently, the overlap ratio can be used to estimate the reproducibility of the ICA results across sessions.

Data Accounted for

To determine the salience of a selected component k in the raw data, its mean back-projected time course over the ROA voxels in the original data space ($X_{k|ROA}$) was compared to the mean ROA time course in the raw data (X_{ROA}) by computing the percent variance accounted for by the component (PV_k).

$$PV_k = 100 \times \left(1 - \frac{\mathrm{var}\left(X_{ROA} - X_{k|ROA}\right)}{\mathrm{var}\left(X_{ROA}\right)}\right)$$

3. RESULTS

For each session, components with strongest ROAs in Brodmann areas (BA) 17, 18, and 19 were selected for further analysis. Figure 2a shows the component ROA, Figure 2b plots the BOLD-image time course and Figure 2c gives the time courses of the 3 largest contributing components to the ROA mean for one component (IC28) active in BA17 (V1) in a long-stimulus session from Subject 1. In Figure 2c, the black trace shows the ROA mean time course obtained by averaging the time courses of the voxels within the IC28 ROA (Figure 2a). The red trace reveals the mean ROA time course obtained by back-projecting the defining component (IC28) to the raw data space. It accounts for 79.5% of the variance in the raw data ROA mean. Other components also contribute to the ROA mean, but not strongly, the strongest are shown in blue and green. The time course of the defining component (red trace) was segmented into ten 30-s trials, color-coded and stacked in trial order to form a BOLD- image plot (Figure 2b).

Within subjects, the active maps of the components highlighting the activation in V1 areas were stable across sessions (O_R was 87.2% between long-stimulus sessions and 82.1% between long- and short-stimulus sessions), presumably, because the active area of primary visual cortex was the same in each session. However, the time courses of hemodynamic

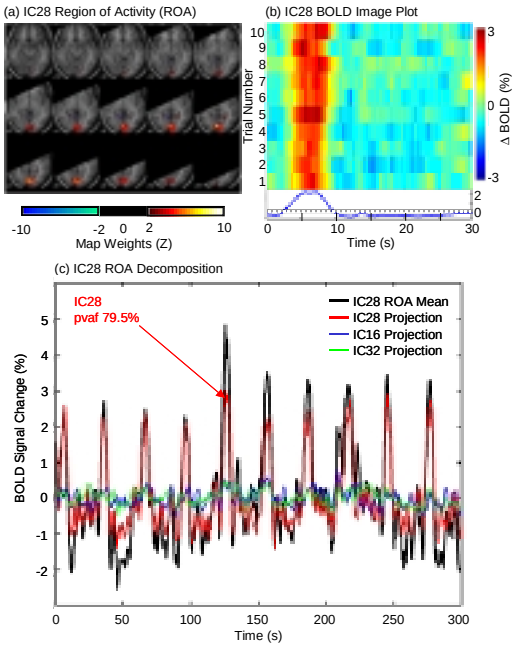

Figure 2 BOLD image for an independent component localized to visual cortex. It shows: (a) region of activity (ROA) determined by independent component (IC) 28 from the decomposition of a long-stimulus session of Subject 1; (b) BOLD-image plot of IC 28 time course; and (c) ROA mean time course by averaging the time courses of voxels in the ROA (black trace) and the time course of IC 28 (red trace) determined by back-projecting the ICA component to original voxel space.

activity of these components differed markedly across trials, sessions, and stimulus types. In later trials of short-stimulus sessions, the V1 component time course contained two major peaks separated by ~17 s with varying latency, while the single-trial HRs for the corresponding component in long-stimulus sessions contained only one peak of larger amplitude and longer duration. As expected, the regional percent signal change in the component ROA was larger on long-stimulus sessions than short-stimulus sessions.

The top panel of Figure 3 shows ROAs of components active in area V1 for the other five subjects. The middle and lower panels show the corresponding BOLD-image plots for the short- and long-stimulus sessions, respectively. The active pari-calcarine regions varied slightly between subjects (possibly, in part, from the slightly different viewing angle for each subject). The BOLD-image plots, however, reveal that the HR time courses of the V1 components varied widely between subjects and within sessions, across trials. For clearer presentation, the BOLD-image plots in Figure 3 were smoothed with a vertical two-trial moving window, and were color coded with individually fit color scales.

4. DISCUSSION

We have shown that BOLD responses to simple, infrequent presentations of flickering checkerboard stimuli may have differing time courses across single trials, stimulus parameters, experimental sessions and subjects. To show this, we introduced a new method of plotting event-related BOLD time courses, the BOLD-image plot, which can clearly visualize

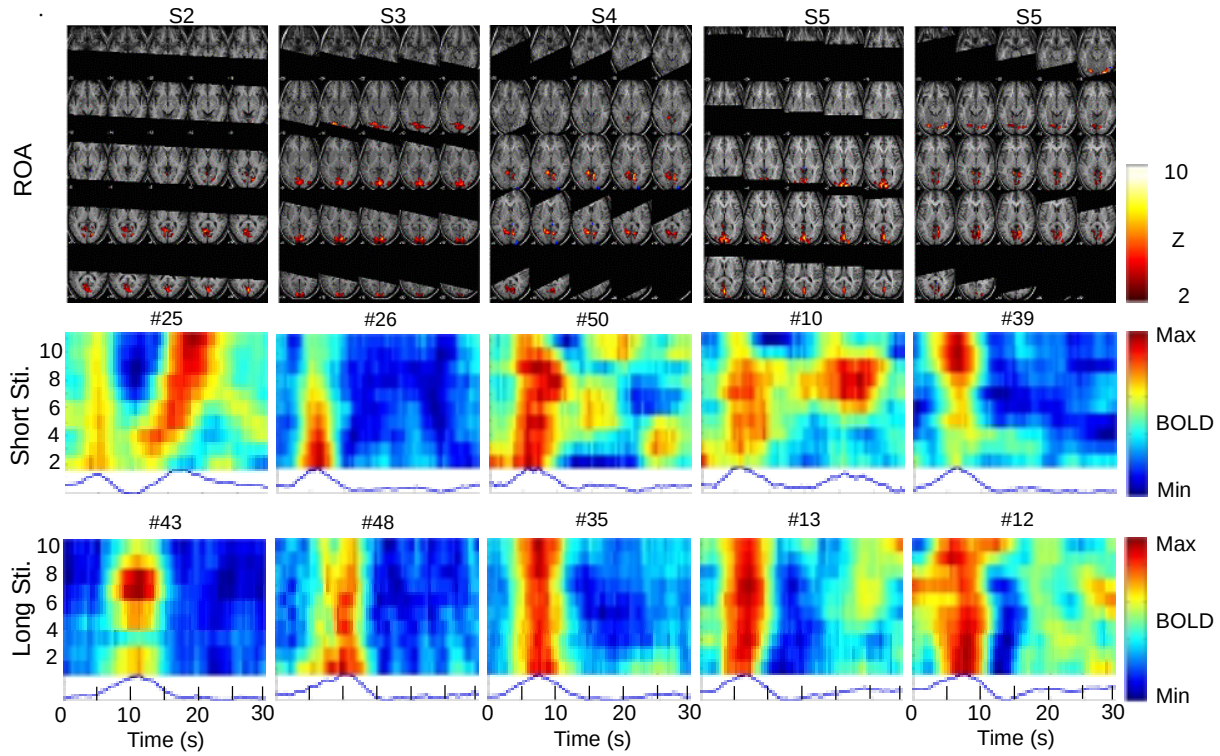

Figure 3 BOLD images from five subjects showing comparison between independent components with similar brain localization. The upper block shows the component ROA map in V1 area of each subject. Middle block displays the BOLD-image plot of the component time course of the short-stimulus session and the lower block the long-stimulus session.

single-trial variations in event-related HRs. BOLD-image plotting should also prove useful for plotting event-related BOLD HRs for single voxels or any other region of interest (ROI). We used ICA decomposition of the data to show that:

1. Active sensory areas may be similar across stimulus parameters.

For each subject, the independent component ROAs activated in V1 following short and long stimulus bursts, determined in separate ICA decomposition for each session, were highly replicable within subjects but differed between subjects, consistent with the report of Waldvogel et al. who used similar stimuli and analyzed their data using co correlational methods [33].

2. HRs to simple stimuli in sensory brain areas may be surprisingly variable.

Many fMRI studies have reported that changes in the subject performance strategy, habituation, learning or aging can produce larger spatiotemporal differences in the BOLD signals recorded from the same subject performing the same task [22,34]. Expected hemodynamic responses might even be completely missing in some trials, reducing the statistical power of fixed models or templates [35]. Methods based on assumptions that HRs are reliably evoked by each stimulus, such as deconvolution approaches that separate HRs from BOLD data using the stimulus presentation record, ignore the possibility that BOLD signals may not be the passive convolution of expected neural activity patterns with a fixed HR kernel. Such methods make the questionable assumptions that the time course of brain metabolism can be predicted from the stimulus or event sequence, and that the HR convolution process is static.

ICA, on the other hand, makes no assumptions about either the shape of HRs or their consistency across trials. It does not rely on a convolutional model or assume that hemodynamic signals represent a fixed low-pass filter applied to neural activity levels. It is able to detect and separate functional brain areas with coherent BOLD time courses, even if omitted or multiple HRs occurs. For example, applied to our data from short-stimulus sessions, ICA detected V1 component HRs exhibiting two peaks in most trials. In these sessions, the first peak was more or less time-locked to stimulus onsets, while the second peak varied in amplitude and latency across trials and sessions. In long-stimulus sessions, the HR of the component located in the same cortical areas contained only a single peak of larger amplitude and longer duration. It would have been difficult for us to discover these phenomena by searching through the data using a wide variety of conceivable but otherwise unmotivated HR templates. Furthermore, the statistical power of such a search would be dissipated to its many degrees of freedom, making confidence in the results questionable.

Based on these results, the sufficiency of the convolution model for sensory-driven HRs, and of results derived from it, should be reconsidered. At least the actual time courses of identified active regions should be checked using BOLD-image plots for variability not easily attributable to a constant noise background.

3. HRs to visual stimuli can vary widely between sensory areas.

While comparing the results in Figure 3 the time courses of the active V1 components differed from those of the MT/V5 components, even within the same subject and session. In area V1, HRs with a first and sometimes a second peak were common. Time courses of MT/V5 components were far less distinct and regular. This difference appears compatible with the hierarchic organization of the visual system. In the visual M-pathway, feed-forward information flows from V1 through

V2 and MT/V5 to the posterior parietal cortex. Since MT/V5 integrates activity from other brain areas for motion detection [36,37], its hemodynamics might be more context dependent than that in V1.

4. HRs can vary between subjects, even in primary sensory areas.

Causal comparison of the active component maps, BOLD-image plots and averaged time courses for V1 components in Figure 3 reveals clear between-subject HR variability in spatial location and time course of the active regions. If it is necessary for group analysis to combine results from different subjects, for V1 or other areas, this variability could diffuse the resulting mean spatial map and time course, leading to Type I errors. Extra caution should thus be exercised during subject group analysis based on map or time course averaging. It should also be expected that the quantity and quality of HR variability should increase in non-primary sensory, particular in frontal brain areas.

5. HRs can vary with subject strategy changes or attention shifts.

It is possible that ICA results may uncover unpredicted changes in the direction of attention or task strategy of the subject during the experiment. Although the flickering checkerboard stimuli we used sometimes triggered activation in MT/V5, in the first five trials of the short-stimulus session of Subject 5 (Figure 3, right column) the activation was small or absent. In later trials of the same session, the stimulus-evoked activation was more substantial, dominating the average time course shown below the BOLD image. This difference might reflect top-down influence, such as the subject paying increasing attention to the motion aspect of the stimulus in later trials. It seems probable that top-down influences may contribute strongly to BOLD signal variability, although collecting behavioral or self-report evidence to examine these influences may be challenging.

Usefulness of ICA for BOLD signal decomposition

Conventional hypothesis-driven or model-based methods for analyzing fMRI data require *a priori* knowledge of the HR time course, and are not suitable for finding or measuring HRs with unknown or variable time courses. Variable HRs might be produced by differences in the time course of blood drainage, by either deliberate or unwitting changes in subject performance strategy, by changes associated with learning or habituation, by variations in subject arousal, attention or imagination, and/or by other unknown hemodynamic or artifactual processes. In such cases (which might indeed prove to be the norm), ICA provides an effect data-driven method for separating the recorded BOLD signals into components accounting for activity of different brain processes, without relying on restrictive assumptions concerning the forms of the HR time courses or the spatial configurations of the active areas.

The main spatial assumption used by Infomax ICA – that small brain regions with mainly coherent BOLD time courses have substantially separate regions of activity – appears physiologically reasonable and non-restrictive. However, if the ROA of an active functional area changes across the training data, as with learning, ICA may separate its activity into consistently-active and transiently-active components with adjoining ROAs, a possibility that can easily be checked by careful component comparison. Similar component splitting might occur if BOLD activity saturated the signals from the most active voxels in a component ROA. Thus, as with any analysis method, the results of ICA can only be as definitive as the goodness of fit between the assumptions of the method and the data.

5. CONCLUSIONS

We have shown that brain HRs to sensory stimuli in an unstructured perception task may be time varying and site-, stimulus- and subject-dependent. In general, the assumption that a fixed combination of template functions can accurately map task-related brain areas and extract their time courses in the same or different brains is questionable. Relying on template-based methods requires two leaps of faith. The first is that the temporal relationship between the task or stimulus sequence and brain metabolic activity is known and can be used to construct a response template. The second is that the brain hemodynamic system acts as a static and, therefore, passive low-pass filter with a fixed or highly constrained impulse response.

The use of ICA can complement hypothesis-driven methods for analyzing fMRI time series because: (1) ICA does not rely on *a priori* knowledge of HR time courses and can be used to detect unforeseen, time varying and site dependent HRs. (2) ICA can be used to separate the component processes corresponding to task-related metabolic responses, non-task related physiological phenomena, and machine and movement artifacts [8-10]. In particular, ICA might be able to reveal changes in the psychological state of subjects or patients. For example, it should allow the characterization of changes in subject performance with learning or habituation. Since ICA can separate a wide variety of time courses contained in fMRI time series, it also should expand the possible types of fMRI experiments that can he performed and meaningfully analyzed and interpreted.

The exploration of nonstationary responses with ICA should allow fMRI research to move beyond fixed signal plus noise models of BOLD dynamics, and to consider the relationship between BOLD signal variability and shifting cognitive states that depend on motivation, arousal and intent.

6. REFERENCES

[1] Ogawa, S., Tank, D., Menon, R., Ellermann, J., Kim, S., Merkle, H., Ugurbil, K. 1992: Intrinsic signal changes accompanying sensory stimulation: functional brain mapping with magnetic resonance imaging. *Proc. Natl. Acad. Scr. USA.* **89**: 5951-5959.

[2] Kwong, K., Belliveau, J., Chesler, D., Goldberg, I., Weisskoff, R., Poncelet, B., Kennedy, D., Hoppel, B., Cohen, M., Tunner, R., Cheng, H.-M., Brady, T., Rosen, B. 1992: Dynamic magnetic resonance imaging. *Proc. Natl. Acad. Sci. USA.* **89**: 5675-5679.

[3] Bandettini, P., Jesmanowicz, A., Wong, E., Hyde, J. 1993: Processing strategies for time-course data sets in functional MRI of human brain. *Magn. Reson. Med*. **30**: 161-173.

[4] Bandittini, P. A., Kwong, K. K., Davis, T. L., Tootell, R. B. H., Wong, E. C., Fox, P. T., Belliveau, J. W., Weisskoff, R. M., Rosen, B. R. 1997: Characterization of cerebral blood oxygenation and flow changes during prolonged brain activation. *Hum. Brain Mapping* **5**: 93-109.

[5] Friston, K. 1995: Commentary and opinion: II. Statistical parametric mapping: Ontology and current issues. *J. Cereb. Blood Flow Metab*. **15**: 361-370.

[6] Friston, K. J., 1997: *Trend Cog. Sci.*

[7] Moeller, J., Strother, S. 1991: A regional covariance approach to the analysis of functional pattern in positron emission tomography data. *J. Cereb. Blood Flow Metab.* **11**: A121-A135.

[8] McKeown, M. J., Jung, T.-P., Makeig, S., Brown, G. G., Lee, T.-W., Kindermann, S. S., Sejnowski, T. J. 1998: Spatially independent activity patterns in functional MRI data during

the Stroop color-naming task. *Proc. Natl. Acad. Sci. USA.* **95**: 803-810.
[9] McKeown, M. J., Makeig, S., Brown, G. G., Jung, T.-P., Kindermann, S. S., Bell, A. J., Sejnowski, T. J. 1998: Analysis of fMRI data by blind separation into independent spatial components. *Hum. Brain Mapping* **6**: 160-188.
[10] McKeown, M. J., Sejnowski, T. J. 1998: Independent component analysis of fMRI data: Examining the assumptions. *Hum. Brain Mapping* **6**: 368-372.
[11] Rajapakse, J. C., Kruggel, F., Maisog, J. M., von Cramon D. Y. 1998: Modeling hemodynamic response for analysis of functional MRI time-series. *Hum. Brain Mapping* **6**: 283-300.
[12] Kruggel, F., von Cramon, D. Y. 1999: Modeling the hemodynamic response in single-trial functional MRI experiments. *Magn. Reson. Med.* **42**: 787-797.
[13] Kruggel, F., von Cramon, D. Y. 1999: Temporal properties of the hemodynamic response in functional MRI. *Hum. Brain Mapping* **8**: 259-271.
[14] Josephs, O., Turner, R., Friston, K. 1997: Event-related fMRI. *Hum. Brain Mapping* **5**: 243-248.
[15] Zarahn, E., Aguirre, G., D'Esposito, M. 1997. A trial-based experimental design of fMRI. *Neuroimage* **6**: 122-138.
[16] Friston, K. J., Fletcher, P., Josephs, O., Holmes, A., Rugg, M. D., Turner, R. 1998: Event-related fMRI: Characterizing differential responses. *Neuroimage* **7**: 30-40.
[17] Gjedde, A. 1997: The relation between brain function and cerebral blood flow and metabolism. Cerebrovascular Diseases, Lippincott-Raven, Philadelphia.
[18] Frahm, J., Merboldt, K., Hanicke, W., Klenschmidt, A., Boecker, H. 1994: Brain or vein oxygenation or flow? On signal physiology in functional MRI of human brain activation, *NMR Biomed.* **7**: 45-53.
[19] Lee, A., Glover, G., Mayer, G. 1995: Discrimination of large venous vessels in time-course spiral blood-oxygenation-dependent magnetic resonance function neuroimaging. *Magn. Reson. Med.* **33**: 745-754.
[20] Kansaku, K., Kitazawa, S., Kawano, K. 1998: Sequential hemodynamic activation of motor areas and the draining veins during finger movements revealed by cross-correlation between signals from fMRI. *Neuroreport* **9**: 1969-1974.
[21] Aguirre, G. K., Zarahn, E., D'Esposito, M. 1998: The variability of human, BOLD hemodynamic responses. *Neuroimaging* **8**:360-369.
[22] Williams L. M., Brammer, M. J., Skerrett, D., Lagopolous, J., Rennie, C., Kozek, K., Olivieri, G., Peduto, T., Gordon, E. 2000: The neural correlation of orienting: an integration of fMRI and skin conductance orienting. *NeuroReport* **11**: 3011-3015.
[23] Andino, S. L. G., de Peralta Menendez, R. G., Thut, G., Spinelli, L., Blanke, O., Michel, C. M., Seeck, M., Landis, T. 2000: Measuring the complexity of time series: an application to neurophysiological signals. *Hum. Brain Mapping* **11**: 46-57
[24] Clare, S., Humberstone, M., Hykin, J., Blumhardt, L. D., Bowtell, R., Morris P. 1999: Detection activations in event-related fMRI using analysis of variance. *Magn. Reson. Med.* **42**: 1117-1122.
[25] Makeig, S., Westerfield, M., Jung, T.-P., Covington, J., Townsend, J., Sejnowski, T. J., Courchesne, E. 2000. Functionally independent components of the late positive event-related potential during visual spatial attention. *J. Neurosci.* **19**: 2665-2680.
[26] Bell, A. J., Sejnowski, T. J. 1995: An information-maximization approach to blind separation and blind deconvolution, *Neural Compu*. **7**: 1129-1159.
[27] Buckner, R. L. 1998: Event-related fMRI and the hemodynamic response. *Hum. Brain Mapping* **6**: 373-377.
[28] Buckner, R. L., Koutstaal, W., Schacter, D. L., Wagner, A. D., Rosen, B. R. 1998a: Functional – anatomic study of episodic retrieval using fMRI. I. Retrieval effort versus retrieval success. *Neuroimaging* **7**: 151-162.
[29] Buckner, R. L., Koutstaal, W., Schacter, D. L., Dale, A. M., Rotte, M., Rosen, B. R. 1998b: Functional – anatomic study of episodic retrieval. II. Selective averaging of event-related fMRI trials to test the retrieval success hypothesis. *Neuroimaging* **7**: 163-175.
[30] Dale, A. M. 1999: Optimal experimental design for event-related fMRI. *Hum. Brain Mapping* **8**: 109-114.
[31] Makeig, S. et al. 1998: MATLAB Toolbox for Independent Component Analysis. *http://www.cnl.salk.edu/~scott/ica.html*.
[32] Jung, T.-P., Makeig, S., McKeown, M. J., Bell, A. J., Lee, T.-W., Sejnowski, T. J. 2001. Imaging brain dynamics using independent component analysis. *Proc. IEEE*. (in press)
[33] Waldvogel, D., van Gelderen, P., Immisch, I., Pfeiffer, C., Hallett, M. 2000: The variability of serial fMRI data: Correlation between a visual and a motor task. *NeuroReport* **11**: 3843-3847.
[34] D'Esposito, M., Zarahn, E., Aguirre, G. K., Rypma, B. 1999. The effect of normal aging on the coupling of neural activity to the bold hemodynamic response. *Neuroimage* **10**: 6-14.
[35] Miezin, F. M., Maccotta, L., Ollinger, J. M., Peterson, S. E., Buckner, R. L. 2000. Characterizing the hemodynamic response: Effects of presentation rate, sampling procedure, and the possibility of ordering brain activity based on relative timing. *Neuroimage* **11**: 735-759.
[36] Zeki, S. 1993: Chapter 20: The P and M pathways and the 'what and where' doctrine. A Vision of the Brain. Blackwell Scientific Publications. London.
[37] Rees, G., Friston, K., Koch, C. 2000: A direct quantitative relationship between the functional properties of human and macaque V5. *Nat. Neurosci.* **3**: 716-723.